

Lifting the fog—a case for non-reversible “lifted” Markov chains

Gabriele Tartero^a, Sora Shiratani^b, and Werner Krauth^{a,c,1}

^aLaboratoire de Physique de l'École normale supérieure, ENS, Université PSL, CNRS, Sorbonne Université, Université Paris Cité, Paris, France; ^bDepartment of Physics, The University of Tokyo, Tokyo, Japan; ^cRudolf Peierls Centre for Theoretical Physics, Clarendon Laboratory, Oxford OX1 3PU, UK

This manuscript was compiled on March 18, 2026

Phase transitions appear all over science, and are familiar from everyday life, as water boiling, sugar melting into caramel or as nematic molecules turning smectic in liquid-crystal displays. The dynamics of phase transitions can be extremely slow, as for example when fog in winter does not lift, that is when the coarsening takes much time from many tiny water droplets to fewer but larger rain drops that feel the pull of gravity. The dynamics of phase transitions is relevant also for the performance of computer algorithms, whose time evolution is often patterned after physical processes. In the ubiquitous Metropolis Monte Carlo algorithm, the mixing dynamics towards equilibrium leads towards the solution of a sampling problem. It is governed by the same reversibility and detailed-balance principles as the overdamped physical dynamics of fog. In the example of the phase-separated Lennard-Jones system, we describe here how the coarsening dynamics of non-reversible “lifted” variants of the Metropolis algorithm proceeds on much faster time scales, with the microscopic non-reversibility translating into large-scale relative motion of droplets that is impossible under the Ostwald-ripening condition of reversibility. A density–displacement coupling moves droplets relative to each other through a lensing effect. Efficient implementations of the long-range Metropolis algorithm and its non-reversible lifting (event-chain Monte Carlo) allow us to show that, in consequence, the coarsening growth exponent is larger under lifting. For large system sizes, the computing problem is thus solved infinitely faster than before, with the outcome (the equilibrium state) strictly unchanged with respect to the Metropolis algorithm. We also discuss the larger setting of our findings, namely that “lifted” non-reversible algorithms can be set up for generic reversible sampling methods, with applications going much beyond our example of lifting fog.

Phase transitions | Coarsening | Markov chains | Ostwald ripening | Non-reversibility

For a range of temperatures and volumes, the equilibrium state of a system of N particles may be composed of two coexisting phases, following their separation at a first-order transition. During a cool night, for example, part of the water vapor contained in air may nucleate into tiny liquid droplets, creating fog. In spite of its persistence in time, familiar to every reader of 19th century English novels, fog is far from being an equilibrium state: It is unstable at large times. The explanation for this inescapable fact is that Nature strives to minimize free energy and that a single drop has smaller surface and lower surface free energy than two droplets of same combined volume. Eventually, droplets must thus coalesce until (in a finite volume) they form a single approximately spherical drop or until they precipitate as rain under the action of gravity (see Fig. 1). The persistent and apparently paradoxical Dickensian fog of *Bleak House* (1), sticking around for days, illustrates that the coarsening dynamics of droplets increasing in size and decreasing in number is excruciatingly slow. Fog practically never precipitates into rain, and it generally lifts through a change of the external parameters: with an increase in temperature or with wind that starts to blow. After a while, a new equilibrium state is attained at a different temperature, without the original phase separation.

Computational science patterns many of its techniques after physical processes. Thus, molecular dynamics and gradient descent mimic Newtonian time evolution in applications from physics to machine learning, and the vast field of Monte Carlo sampling, pioneered in physics by Metropolis et al. in 1953, now permeates all of science. The Metropolis algorithm, one of the most cited works in science (2), is a black box for computing and is perceived as a panacea for arbitrary sampling problems. The Metropolis algorithm implements time-reversible dynamics that converges towards equilibrium. The time reversibility, in other words the detailed-

Significance Statement

The Metropolis algorithm, as many mainstays of computational science, is patterned after physical dynamics, and it thus time-reversible. We discuss the limitations that arise from reversibility, and how they are overcome through non-reversible “liftings”. In the Lennard-Jones liquid, where reversibility necessarily leads to slow Ostwald ripening in the coarsening dynamics towards equilibrium, we describe a lensing effect that induces relative motion of macroscopic droplets in the lifted algorithm, namely event-chain Monte Carlo. A highly efficient implementation for long-range interactions allows us to demonstrate an increased coarsening growth exponent and thus a reduced scaling for the mixing time. Therefore, for large system sizes, the lifted algorithm converges infinitely faster than the original reversible one. Our findings explain recent successes of event-chain Monte Carlo and point to future applications of non-reversible Markov chains in computational science and applications.

Author affiliations: ^aLaboratoire de Physique de l'École normale supérieure, ENS, Université PSL, CNRS, Sorbonne Université, Université Paris Cité, Paris, France; ^bDepartment of Physics, The University of Tokyo, Tokyo, Japan; ^cRudolf Peierls Centre for Theoretical Physics, Clarendon Laboratory, Oxford OX1 3PU, UK

¹To whom correspondence should be addressed. E-mail: werner.krauth@ens.fr

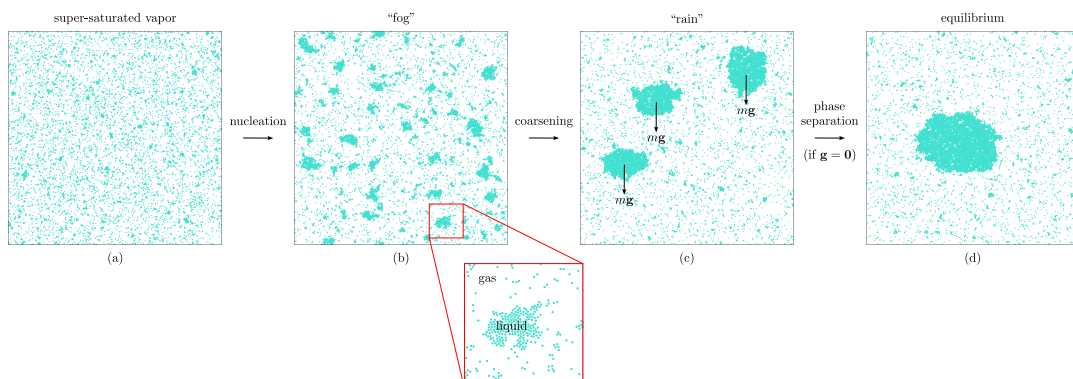


Fig. 1. Coarsening of the two-dimensional Lennard-Jones system ($N = 10^4$ particles at density $\rho = 0.1$) from super saturation (a) into a single liquid drop surrounded by vapor (d). After nucleating several droplets (b), the system goes through a coarsening process, that gradually reduces the number of liquid clusters while increasing their average size (c). In the absence of gravity, the equilibrium state contains a single floating drop. The Metropolis algorithm, that mimics the physics of Ostwald ripening, needs about 10^{12} steps to complete this process, while its lifted counterpart, event-chain Monte Carlo, reaches equilibrium after around 10^9 events.

balance condition, built into the algorithm in or out of physics, is identical to the governing principle of the fog dynamics of tiny droplets. In very general applications, the Metropolis algorithm will, so to speak, eventually turn small droplets into rain, but the mixing time (3) for this to come to fruition can be enormous, just as for the “fog everywhere” in “implacable November weather” (1, p.12). Two aspects of the analogy with London fog are crucial: First, the equilibrium state encoded in the Metropolis algorithm represents the solution of a given computational problem, and we require a speed-up of the dynamics without changing the steady state (without having the sun dissipate the fog). Second, in the case of a two-phase mixture, it has been understood since Ostwald in the late 1800s that a configuration with several droplets cannot be stationary, thus providing a clear-cut criterion for stationarity. In general, however, it is very difficult to ascertain that the steady state has been reached. This risks flawed conclusions, as for example in Fig. 1b (if we lacked Ostwald’s insight), which is “almost” stationary under local reversible dynamics, but which is not at all in equilibrium (represented by Fig. 1d).

Non-reversible (thus, effectively, non-equilibrium) Markov chains violate detailed balance, and they feature finite steady-state flows even if the steady state is the equilibrium Boltzmann distribution. The perceived paradox of non-equilibrium in equilibrium has been clarified in exactly solved models (4, 5). The practical construction of non-reversible Markov chains with an imposed steady state has long lacked clear design principles, but the concept of “lifting”, which copies every configuration of a parent chain into multiple configurations, has allowed definite progress (6, 7). An example of non-reversible lifted Markov chains is given by the event-chain Monte Carlo algorithms for particle systems whose Boltzmann distributions then appears as a stationary state with finite flows (8, 9).

The characteristic convergence times for lifted Markov chains obey mathematical constraints (7). First, in order to speed up a reversible parent Markov chain, its lifting must be non-reversible. This validates our intuition that the slow evaporation of liquid particles from a small droplet into the vapor and the condensation of vapor particle to a larger liquid droplet (Ostwald ripening (10, 11)) explains the persistence of fog, and more generally the slowness of the local Metropolis

algorithm. Second, the convergence times of a lifted Markov chain are lower bounded by the square root of the times of its reversible parent algorithm. This validates the concept of ballistic vs. diffusive motion for general Markov chains, much beyond the realm of particle systems. However, the lower bound does not guarantee that non-reversibility at a microscopic level actually speeds up convergence. Up to now, it has remained unclear whether a speed-up beyond a size-independent factor can be obtained in real-life many-particle systems beyond one dimension.

In this paper, we first discuss reversible and non-reversible Markov chains, with, in the case of long-range-interacting particle systems, the (factorized) Metropolis algorithm as an example of the former and event-chain Monte Carlo of the latter. Second, we analyze how event-chain Monte Carlo accelerates the coarsening dynamics of a two-dimensional Lennard-Jones system through fast relative motion of liquid droplets, what the Metropolis algorithm cannot achieve. The limitations of Ostwald ripening are overcome by a density-velocity coupling that induces macroscopic motion of droplets with respect to each other. A related coupling has been analyzed rigorously in a one-dimensional context (12). Third, we provide highly optimized open-source implementations of these algorithms, to rigorously simulate cutoff-free Lennard-Jones particle systems. This allows us to quantify the above effects and to show that, on a macroscopic scale, they lead to a better coarsening growth exponent for this process (characterizing the mean droplet size as a function of time). We relate the coarsening growth exponent to the much improved scaling of the mixing time with system size. In the conclusions, we review from a larger perspective why non-reversibility is responsible for the improved scaling and the infinite speedup of the non-reversible algorithm for large systems. We discuss possible applications of our findings in statistical physics, and extensions to chemical physics and to machine learning.

Reversible and non-reversible coarsening

In the fog of 19th century London, small droplets move in over-damped (windless) conditions and the Maxwell velocity of macroscopic droplets effectively vanishes, together with all probability flows. The detailed-balance dynamics is time-reversible, just as the Metropolis algorithm. To showcase re-

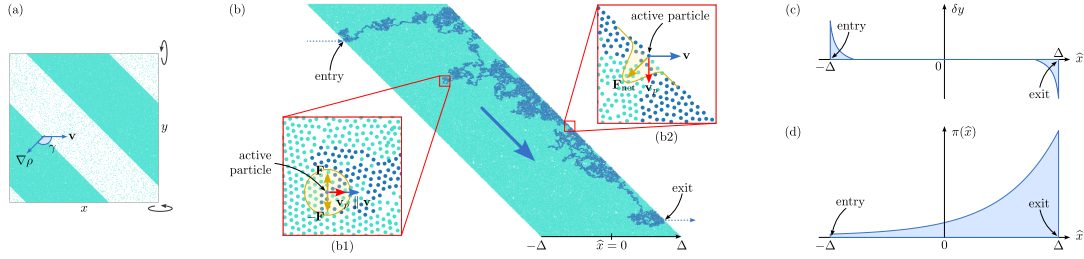


Fig. 2. Density–velocity coupling of event-chain Monte Carlo in a periodic liquid ribbon. (a): The ribbon in its periodic simulation box ($\sim 10^5$ liquid particles at density $\rho = 0.75$ surrounded by vapor, see Supplementary Material for details). The event chain’s direction of motion is towards the right ($+x$) (b): Typical event chain, from its entry into the ribbon to its exit from it. (b1): Inside the ribbon, the active particle interacts—and the event chain grows—symmetrically around the direction of motion. (b2): At the ribbon boundary, the active particle interacts symmetrically around the density gradient and the event chain grows with a component perpendicular to the direction of motion (here, in the $-y$ direction). (c): Mean vertical growth component δy of the event chain as a function of its horizontal position $\hat{x} \in [-\Delta, \Delta]$ in the ribbon. The opposite boundary effects are due to the opposite sign of the density gradient at the two interfaces. (d): Probability distribution of the active particle’s \hat{x} coordinate. The event chain grows predominantly near the forward boundary, as already evident from (b). The curves in panels (c) and (d) are smoothed, schematic, versions of the plots from the Supplementary Material.

versible and non-reversible coarsening in a model that is easily visualized, we pit against each other the factorized Metropolis algorithm (13) (which is reversible) and the event-chain Monte Carlo algorithm (which is lifted and non-reversible), in the two-dimensional Lennard-Jones model with long-range interactions (see Methods for details on the algorithm and the model parameters). At each time step, the Metropolis algorithm attempts to move a random particle symmetrically around its current position. The lifted algorithm, *mutatis mutandis* makes the same moves but organizes them differently. For a certain time, they are all in the $+x$ direction, then in the $+y$ direction (the moves in $-x$ and $-y$ are not required in a periodic system). After an accepted move of particle i it moves that particle again. Because of the factorization, rejection can always be attributed to a single target particle j . After a move of active particle i rejected by target particle j , it is j that moves next, and in the same direction. After a certain time, the direction of motion switches between $+x$ and $+y$. An additional “factor-field” control parameter (14, 15) of event-chain Monte Carlo will not be explored in this paper.

Event-chain Monte Carlo converges to a NESS (“non-equilibrium steady state”) identical to equilibrium, yet it conserves finite particle and probability flows. Two of our movies illustrate the time evolution from the super-saturated vapor towards phase-separated equilibrium configurations. For the reversible algorithm, macroscopic droplets are essentially immobile, but larger droplets generally grow at the expense of smaller ones that shrink, then disappear, thus realizing Ostwald ripening (see Movie S1 in the Supplementary Material). This is because smaller droplets have a slightly higher particle evaporation rate yet a lower particle adsorption rate than bigger ones. The non-reversible algorithm has droplets move with respect to each other. This allows them to coalesce (see Movie S2). In a system of $N = 10^4$ Lennard-Jones particles at density $\rho = N/L^2 = 0.1$ (corresponding to Fig. 1 and Movies S1, S2 and S3), the coarsening process ends with a single droplet of size $\sim 0.085 \times L^2$ (that is, a radius of $R \simeq 52.0$ in a box of length $L \simeq 316.2$) after $\sim 10^{12}$ individual steps for the reversible Metropolis algorithm and after $\sim 10^9$ steps for non-reversible event-chain Monte Carlo. The steady states of these algorithms are rigorously the same. The speedup is substantial.

Density–velocity coupling of non-reversible dynamics

To analyze the speedup of the coarsening dynamics (Movie 2 compared to Movie 1), we consider the growth of an event chain at a density gradient with inclination angle γ with respect to its direction of motion. For concreteness, we realize the density gradient as an infinite periodic ribbon of liquid surrounded by vapor and take the direction of motion as $+x$ (see Fig. 2a). The active particle i at the head of the event chain moves in $+x$ until its further displacement is opposed by the “target” particle j which in turn becomes active. The target particle is most likely inside the ribbon and in the direction of the density gradient, simply because that is where most candidate target particles are situated. If the ribbon is oriented as in Fig. 2a (that is, for $\pi/2 < \gamma < \pi$), the target particle and, thus, the new head of the event chain will likely be at a lower y . After the entry of the event chain into the ribbon, the chain first grows along the direction of motion, but close to the right boundary, it repeatedly grows in direction of the density gradient, that is, downward (see Fig. 2b). Two aspects of the effect stand out. First, at the back and the front of the ribbon, the event chain is deflected perpendicularly to the direction of motion (Fig. 2c). This creates a macroscopic perpendicular offset of the exit position with respect to the entry point. Second, particles at the front of the ribbon are more likely to participate in the growth of the event chain than particles in its center or at its back (see Fig. 2d). This will end up by destroying the ribbon because particles in the event chain move forward whereas the others do not. It also indicates that the ribbon must be out of equilibrium as, in equilibrium, each particle in the system has the same probability to be active (see Methods).

Lensing

In the ribbon of Fig. 2, the density gradient deflects the event chain perpendicularly to the direction of motion in a way that is strongest when the ribbon is almost parallel to the direction of motion (for an inclination angle $\gamma \gtrsim \pi/2$), and that vanishes when it is almost perpendicular (inclination angle $\gamma \sim \pi$). Inside a spherical liquid droplet, the event chain encounters a varying inclination angle, possibly starting with strong deflection (near the north or south poles in Fig. 3b), then ending close to the tip of the droplet with $\gamma \sim \pi$ and no deflection (see Fig. 3b). This results in a migration of the event chain from the poles towards the tip of the droplet,

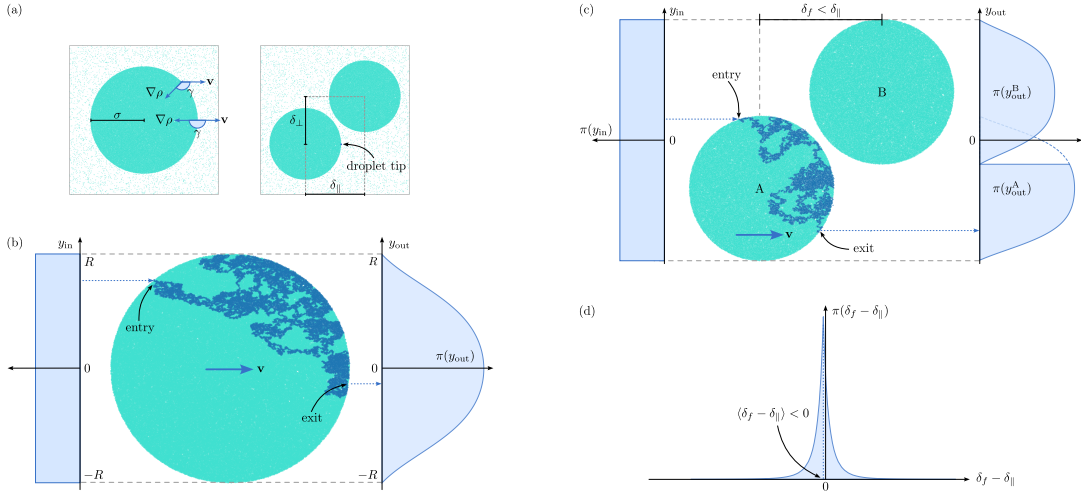


Fig. 3. Lensing effect of event-chain Monte Carlo and relative motion of droplets. (a): Circular liquid droplet of radius R and pair of droplets in their periodic simulation boxes. (b): Lensing effect of event chain Monte Carlo inside a liquid drop. The event chain, entering the drop uniformly undergoes multiple gradient effects and then leaves it predominantly near its tip. (c): Relative motion of two droplets created by the lensing effect. An event chain entering drop A, even at its extremity, likely exits it without touching drop B (see histogram). The expected time spent in A, and thus the displacement of A in $+x$ direction is larger than the time spent in and the displacement of B. (d): Probability distribution of the variation $\delta_f - \delta_{\parallel}$ in the horizontal separation between the droplets. Its negative mean value shows that the two droplets approach each other. The curves in panels (b), (c) and (d) are smoothed versions of histograms from the Supplementary Material.

in other words in a lensing. In our example of the motion in $+x$, a uniform distribution of event-chain entry heights in y produces a distribution of exit heights y that is centered around the symmetry axis (see Fig. 3b). The lensing effect exists for general potentials and even for hard disks. We expect it to depend on the factor-field control parameter of event-chain Monte Carlo.

Relative motion of droplets

Because of the lensing, event chains that enter a droplet A of radius R migrate towards its tip and then exit. The time they spend in droplet A determines how much the latter advances. We consider a second droplet B (also of radius R) in the shadow of A, for a perpendicular pair distance δ_{\perp} smaller than twice the droplet radius ($\delta_{\perp} < 2R$) (see Fig. 3a). The droplet A then advances for a wide choice of entry positions, and the event chain exits without touching B, although it is in its shadow. If any event chain was exiting A exactly at its tip (complete lensing), droplets A and B would on average approach each other for $2R > \delta_{\perp} > R$ and would move away from each other for $R > \delta_{\perp} > 0$. This is because any chain entering droplet A (and advancing it along the direction of motion) would then also enter droplet B. In practice, the effect of the shadowing is obtained by numerical simulation (see Fig. 3b) and different perpendicular distances cause the droplets to more or less move with respect to each other (see Fig. 3(d) for a histogram and Supplementary Material for a discussion of the different possible cases). Lensing thus overcomes the immobility constraint of Ostwald ripening. This effect survives on the longest time scales as can be tested by relaxing a configuration with two equal-sized droplets all the way into equilibrium and by comparing typical evolutions for the factorized Metropolis algorithm and for event-chain Monte Carlo (see Fig. 4).

Coarsening growth exponents

The lensing effect of event-chain Monte Carlo has consequences at the largest length and time scales, as evidenced in its coarsening dynamics, in other words in the growth with time of the mean radius $\langle R \rangle$ of liquid droplets surrounded by vapor. During coarsening (after the nucleation of many tiny droplets from the super-saturated vapor), the evolution of the mean radius generally follows a power law $\langle R \rangle \propto t^{\alpha}$, where $\alpha > 0$ is the growth exponent. When coarsening proceeds by evaporation of single particles from smaller immobile droplets and condensation of single particles onto larger immobile ones (Ostwald ripening), the coarsening growth exponent is $\alpha = 1/3$ both in two and three dimensions (10, 11, 16, 17). We indeed observe a very small growth exponent close to the theoretical value in our Lennard-Jones model for the Metropolis algorithm (see Fig. 5). The lack of mobility of droplets is readily evidenced in Movie S1. Similar behavior was also numerically verified for the two-dimensional Ising model under Metropolis dynamics (18).

The event-chain Monte Carlo dynamics allows for the macroscopic motion of the droplets themselves. This leads to a larger growth exponent, whose value is influenced by the strength of the lensing effect. For well-chosen values of the chain length l_c , the growth exponent increases significantly, thus making event-chain Monte Carlo infinitely faster than Metropolis in the thermodynamic limit (see Fig. 5). We may identify the time to arrive at a single droplet of size $\propto L$ with the mixing time of the Markov chain: $\langle R \rangle \sim (t/N)^{\alpha}$. For $R \sim L$, thus $\langle R \rangle^{1/\alpha} \sim t/L^2$, we then reach,

$$t_{\text{mix}} \sim L^{2+1/\alpha}. \quad [1]$$

Here, the term in L^2 (which is specific to two spatial dimensions) reflects that we count time in single displacements rather than in sweeps. A larger coarsening growth exponent then implies an improved scaling of the mixing time. The empirical growth exponent varies with l_c , likely because the latter influences the lensing. Too small l_c do not allow the

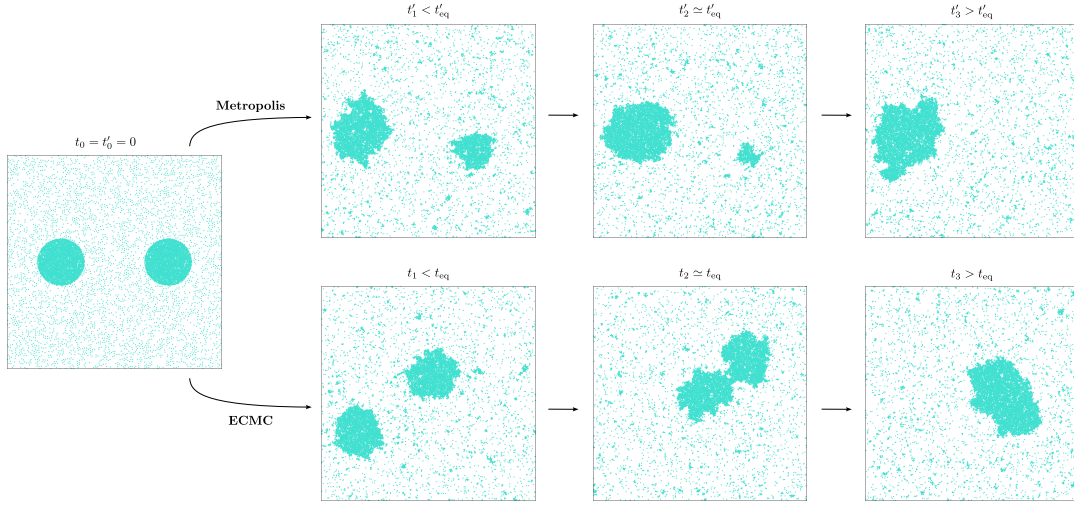


Fig. 4. Equilibration dynamics of the factorized Metropolis algorithm and of event-chain Monte Carlo from an initial configuration with two spherical droplets (with 2565 particles each, at local density $\rho = 0.75$) surrounded by 3872 vapor particles at local density $\rho = 0.05$, and overall density $\rho = 0.1$. Under the Metropolis dynamics, the system equilibrates through Ostwald ripening, that is, through the evaporation–condensation of vapor at the surface of immobile liquid droplets (here, after around 10^{11} moves). Under event-chain Monte Carlo dynamics, the two droplets move relative to each other, allowing them to coalesce much faster (here, after about 10^8 events). We attribute this acceleration to the lensing effect.

chain to grow and a sufficient number of particles to be displaced inside a droplet. On the other hand, too large l_c would hinder the relative droplet displacement due to periodic boundary conditions. In the present paper, we only consider implementations where l_c is fixed throughout the simulation. A dynamically changing $l_c(t) \sim R(t)^2$ (which visits one droplet per chain) may lead to smaller mixing times than a fixed chain length $l_c \sim N$, which might furthermore be influenced by factor fields. Nucleation precedes coarsening on a time scale (in our units) of L^2 , which is asymptotically negligible compared to the coarsening time scale.

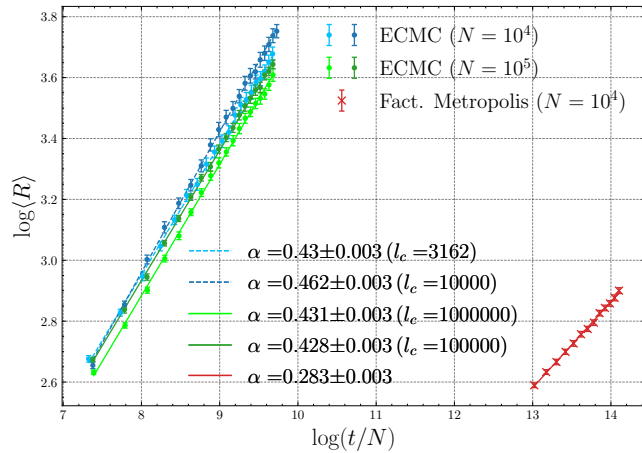


Fig. 5. Coarsening dynamics of event-chain Monte Carlo and factorized Metropolis for a two-dimensional Lennard-Jones system in the phase-coexistence regime ($\rho = 0.1$). The average droplet radius $\langle R \rangle$ depends on time as a power law of growth exponent α , with the time t corresponding to the total distance traveled by all particles in the system. Event-chain Monte Carlo outperforms Metropolis both in terms of scaling and of absolute CPU time. Yet, for finite systems, the growth exponent α is found to depend on the event-chain length. Roughly, event-chain Monte Carlo mixes 100 times faster than the factorized Metropolis algorithm for $N = 10^4$, and 1000 times faster for $N = 10^5$.

Non-reversible steady-state dynamics

The out-of-equilibrium dynamics of event-chain Monte Carlo, as we have demonstrated for specific initial configurations as the ribbon and the spherical droplet, leads to an inhomogeneous growth of event chains, and to an inhomogeneous probability distribution of active particles. It is this inhomogeneous distribution which causes the lensing and which allows the algorithm to overcome the limitations of Ostwald ripening. In equilibrium, the probability distribution of the active particles over the system is uniform, by construction principle for lifted Markov chains (see Methods for a discussion). In consequence, the motion of the single remaining liquid comes to a still-stand, and it hardly moves with respect to the surrounding vapor (see Movie S3). This fascinating change of behavior between out-of-equilibrium and equilibrium dynamics links the equilibrium geometry of the liquid–vapor interface to the behavior of event-chain Monte Carlo in a way that is not yet understood.

Conclusion and outlook

In this paper, we have studied the transmission of non-reversibility in local Markov chains from the smallest to the largest length and time scales. In our example of the two-dimensional Lennard-Jones system approaching coexistence, we showed how non-equilibrium density fluctuations influence the mixing dynamics. The relative motion of droplets is a consequence of an intrinsic density–velocity coupling, that arises naturally in lifted algorithms, and that cannot be achieved in reversible Monte Carlo algorithms and neither in molecular dynamics nor in Hamiltonian Monte Carlo (19). The resulting dynamics mixes much faster than the reversible Metropolis algorithm, where droplets barely move and are thus doomed either to evaporate or to grow, until equilibrium is reached. Quantitatively, we were able to show that, during coarsening, event-chain Monte Carlo exhibits a larger growth exponent than Metropolis. As a consequence, its mixing time has better scaling than the reversible one.

Analogous behavior was found in a one-dimensional particle system on a lattice under what amounts to event-chain Monte Carlo dynamics (12). The coupling of density differences to the local velocity there speeds up the mixing dynamics for specific initial configurations as well as the relaxation dynamics for equilibrium density fluctuations. The extension to two spatial dimensions that we presented in this paper is remarkable, and it would be interesting to understand in more general terms the role of the dimension. The lensing effect may well explain the effectiveness of event-chain Monte Carlo algorithms in hard-disk systems (20) which are governed by the physics of coarsening of hexatic droplets in a liquid background rather than that of liquid droplets in a vapor background studied in the present paper. In essence, we have shown here that a non-reversible *local* Markov chain can perform better (100 times for $N = 10,000$, 1000 times for $N = 100,000$) than a reversible *local* Markov chain, in the real-life setting of the Lennard-Jones system. What is gained cannot be achieved with simply replacing reversible Markov chains with molecular dynamics, Hamiltonian Monte Carlo or stochastic gradient descent, as was argued elsewhere (19). We expect applications of non-reversible lifted Markov chains from chemical physics to the vast field of machine learning.

Materials and Methods

Lennard-Jones system. In this paper, we consider a system of N point particles in a periodic two-dimensional square box of size L , interacting via the Lennard-Jones pair potential:

$$U_{\text{LJ}}(r) = 4\epsilon \left[\left(\frac{\sigma}{r} \right)^{12} - \left(\frac{\sigma}{r} \right)^6 \right]. \quad [2]$$

The equilibrium Boltzmann weight of a configuration is $\exp \left[-\beta \sum_{i < j=1}^N U_{\text{LJ}}(r_{ij}) \right]$, where β is the inverse temperature, and r_{ij} is the periodically corrected pair distance between particles i and j . We introduce no cutoff in the model, but nevertheless arrive at efficient reversible and non-reversible implementations (see below for more details). In eq. (2), we set $\sigma = 1$, $\epsilon = 1/0.46$ for every system size, and consider a constant number density $\rho = N/L^2 = 0.1$ for all system sizes. At inverse temperature $\beta = 1$, these values lead to a phase-separated equilibrium state, where the liquid particles are gathered in a single drop of local density $\rho \simeq 0.71$ surrounded by vapor of local density $\rho \simeq 0.04$ (21). To identify the liquid during the time evolution, we coarse-grain the system with a regular grid with cells of volume 100 and classify as “liquid” any cell whose local density is larger than $\rho = 0.5$ (that is, which contains more than 50 particles). A liquid droplet then constitutes a contiguous set of liquid cells of a well-defined coarse-grained two-dimensional area, the square root of which, divided by $\sqrt{\pi}$, we take to be the radius R . The mean radius $\langle R(t) \rangle$ of Fig. 5 takes an average of R over the droplets in a given configuration.

Lifted Markov chains. Lifting (7) connects an original reversible Markov chain, in our case the factorized Metropolis algorithm, with a Markov chain in an augmented space in a way that reorganizes the moves. If the Metropolis algorithm proposes a random (forward or backward, upward or downward) move of a random particle, its lifted version keeps memory of the previous move (say, forward) and of the previous particle i . The original sample space is thus augmented by the direction and by the index of what we refer to in the main text as the “active” particle.

A lifted Markov chain requires the statistical weight of all the “lifted” copies \hat{a} of an original configuration a (that is, the configuration a of particles together with the direction and the index of the active particle) to add up to the statistical weight (the Boltzmann weight) of a . More restrictively, we require all lifted copies \hat{a} of a to have the same equilibrium stationary weight. This

condition makes that if, in Fig. 2b, particles at the boundary of the ribbon are more likely to be active, this ribbon configuration cannot be in equilibrium. In addition to the equal-repartition rule, one requires also that the statistical flows (the stationary weights $\pi(\hat{a})$ multiplied with the transition probabilities $P(\hat{a} \rightarrow \hat{b})$) sum up to the statistical flows between the original configurations a and b . Under these conditions of lifting, it has become possible to systematically construct non-reversible Markov chains. Lifting can reduce mixing and relaxation times of an original Markov chain roughly to their square roots (7, 8), but the lifted Markov chain must then be non-reversible.

Metropolis algorithm with long-range interactions. The traditional Metropolis algorithm proposes moves, in our case displacements of single particles between configurations a and b , such that the move $a \rightarrow b$ is proposed with the same probability as the move $b \rightarrow a$. Moves are accepted on the basis of the relative Boltzmann weights of a and b , that is, in terms of the change of the total energy difference ΔU between b and a . For the long-range pair potential U_{LJ} of eq. (2) ΔU_{LJ} , for a single-particle displacement, has contributions from throughout the system, resulting in a naive complexity $\mathcal{O}(N)$ per single-particle move. As in molecular dynamics, this problem is commonly overcome by cutting off the potential at a finite spatial range, so that the displacement of a single particle impacts only a finite number of nearby pairs of particles. An $\mathcal{O}(1)$ complexity per move is obtained, but the required extrapolations to infinite range are often fraught with uncertainty (22–24). Here, we rather use the factorized Metropolis algorithm (13), which accepts or rejects moves on the basis of a consensus of Metropolis decisions for all pair factors impacted by the displacement of a single particle. The method can be implemented in $\mathcal{O}(1)$ per move without cutoff (25). For all intents and purposes, it agrees with the traditional Metropolis algorithm (see also Ref. (26)). A fast $\mathcal{O}(1)$ implementation derived from an open-source Python code is used in this paper (see below for access to the code).

Event-chain Monte Carlo with long-range interactions. Event-chain Monte Carlo represents a lifting of the factorized Metropolis algorithm in the limit of infinitesimal moves (8). As described in the main text, a sequence of repeated infinitesimal Metropolis moves of a given “active” particle are proposed in a fixed direction, until one such move is rejected. Any rejection is attributed to a definite “target” particle, which then becomes the active one. With periodic boundary conditions, it is only necessary to have moves in the $+x$ and $+y$ direction. To ensure irreducibility, after a certain chain length l_c , a new active particle is randomly sampled and the direction is switched between $+x$ and $+y$. With infinitesimal moves, the algorithm becomes event-driven, and it generates the eponymous event chains. For hard spheres, this amounts to computing the position of the next collision, given the direction of motion (27). For continuous interactions, the lifted factorized Metropolis algorithm allows the target particle to be sampled exactly (13, 28). Remarkably, this allows the new active particle to be sampled with a complexity $\mathcal{O}(1)$ (29, 30). The Boltzmann distribution is sampled without any correction (for an introduction to this method, see Ref. (26)).

Software packages. The numerical simulations for this paper (factorized Metropolis algorithm and event-chain Monte Carlo for the Lennard-Jones system without cutoff) were performed with open-source code. Our implementations are based on the programs provided with Ref. (25). They all have $\mathcal{O}(1)$ per move complexity. Our codes were carefully checked against `JELLYFysh`, an open-source Python application that implements event-chain Monte Carlo for general short- and long-range interactions (31). Our event-chain Monte Carlo program written in the Rust language is available at <https://github.com/EarlMiktea/lj-ecmc.git>.

Supporting information. Our event-chain Monte Carlo simulations of Fig. 3 are complemented in the Supplementary Material by a number of plots for the lensing effect for a single droplet and for the relative motion of pairs of droplets under varying shadowing conditions. In addition, the Supplementary Material also contains three movies that illustrate the different reversible and non-reversible

Monte Carlo dynamics for the two-dimensional Lennard-Jones system. They are as follows:

Movie S1 (“Coarsening dynamics of the factorized Metropolis algorithm”) starts from an all-vapor initial configuration with $N = 10,000$. It then undergoes nucleation and coarsening to arrive at the equilibrium, as in Fig. 1. The total time to arrive at the equilibrium state with a single droplet is $\sim 10^{12}$ moves, that is, $\sim 10^8$ moves per particle. The Ostwald ripening is manifest, as the big droplets hardly move. They grow through the evaporation of single particles from the small droplets into the vapor and the condensation of single vapor particles onto larger droplets.

Movie S2 (“Coarsening dynamics of non-reversible event-chain Monte Carlo”) also starts from an all-vapor initial configuration. Equilibrium is reached through nucleation and coarsening on a much shorter timescale (around 10^5 events per particle). The relative droplet motion manifestly overcomes the limitations of Ostwald ripening.

Movie S3 (“Equilibrium dynamics of non-reversible event-chain

Monte Carlo”) starts from an equilibrated initial configuration. The equilibrium drop hardly moves, in keeping with the basic property of lifted Markov chains which, in equilibrium, displace each particle with the same probability. The difference between the equilibrium (this movie) and non-equilibrium dynamics (Movie S2) is striking.

All movies track particle configurations in a center-of-mass reference frame, where the mean displacement vanishes for all times.

ACKNOWLEDGMENTS. W.K. acknowledges generous support by the Leverhulme Trust. Part of this research was conducted within the context of the International Research Project “Non-Reversible Markov chains, Implementations and Applications”. S.S. thanks the Laboratoire de Physique de l’École normale supérieure for hospitality. G.T. is grateful to Synge Todo and Koji Hukushima for helpful discussions and insights. We thank Kush Patel for help with the efficient implementation of the factorized Metropolis algorithm.

1. C Dickens, *Bleak House*, Oxford World’s Classics ed. S Gill. (Oxford University Press, London, England), (2008).
2. N Metropolis, AW Rosenbluth, MN Rosenbluth, AH Teller, E Teller, Equation of State Calculations by Fast Computing Machines. *J. Chem. Phys.* **21**, 1087–1092 (1953).
3. DA Levin, Y Peres, EL Wilmer, *Markov Chains and Mixing Times*. (American Mathematical Society), (2008).
4. SC Kapfer, W Krauth, Irreversible Local Markov Chains with Rapid Convergence towards Equilibrium. *Phys. Rev. Lett.* **119**, 240603 (2017).
5. FH Essler, W Krauth, Lifted TASEP: A Solvable Paradigm for Speeding up Many-Particle Markov Chains. *Phys. Rev. X* **14** (2024).
6. P Diaconis, S Holmes, RM Neal, Analysis of a nonreversible Markov chain sampler. *Ann. Appl. Probab.* **10**, 726–752 (2000).
7. F Chen, L Lovász, I Pak, Lifting Markov Chains to Speed up Mixing. *Proc. 17th Annu. ACM Symp. on Theory Comput.* p. 275 (1999).
8. W Krauth, Event-Chain Monte Carlo: Foundations, Applications, and Prospects. *Front. Phys.* **9**, 229 (2021).
9. EAJF Peters, Event-Chain Monte Carlo: The global-balance breakthrough. *KIM Rev.* **4**, 02 (2026).
10. I Lifshitz, V Slyozov, The kinetics of precipitation from supersaturated solid solutions. *J. Phys. Chem. Solids* **19**, 35–50 (1961).
11. C Wagner, Theorie der Alterung von Niederschlägen durch Umlösen (Ostwald-Reifung). *Zeitschrift für Elektrochemie, Berichte der Bunsengesellschaft für physikalische Chemie* **65**, 581–591 (1961).
12. B Massoulié, C Erignoux, C Toninelli, W Krauth, Velocity Trapping in the Lifted Totally Asymmetric Simple Exclusion Process and the True Self-Avoiding Random Walk. *Phys. Rev. Lett.* **135**, 127102 (2025).
13. M Michel, SC Kapfer, W Krauth, Generalized event-chain Monte Carlo: Constructing rejection-free global-balance algorithms from infinitesimal steps. *J. Chem. Phys.* **140**, 054116 (2014).
14. Z Lei, W Krauth, AC Maggs, Event-chain Monte Carlo with factor fields. *Phys. Rev. E* **99** (2019).
15. AC Maggs, Non-reversible Monte Carlo: An example of “true” self-repelling motion. *Europhys. Lett.* **147**, 21001 (2024).
16. Q Zheng, JD Gunton, Theory of Ostwald ripening for two-dimensional systems. *Phys. Rev. A* **39**, 4848–4853 (1989).
17. SK Das, S Roy, J Midya, Coarsening in fluid phase transitions. *C. R. Phys.* **16**, 303–315 (2015).
18. S Majumder, SK Das, Domain coarsening in two dimensions: Conserved dynamics and finite-size scaling. *Phys. Rev. E* **81**, 050102 (2010).
19. W Krauth, Hamiltonian Monte Carlo vs. event-chain Monte Carlo: an appraisal of sampling strategies beyond the diffusive regime (2024).
20. EP Bernard, W Krauth, Two-Step Melting in Two Dimensions: First-Order Liquid-Hexatic Transition. *Phys. Rev. Lett.* **107**, 155704 (2011).
21. YW Li, MP Ciamarra, Phase behavior of Lennard-Jones particles in two dimensions. *Phys. Rev. E* **102**, 062101 (2020).
22. B Smit, D Frenkel, Vapor-liquid equilibria of the two-dimensional Lennard-Jones fluid(s). *The J. Chem. Phys.* **94**, 5663–5668 (1991).
23. B Smit, Phase diagrams of Lennard-Jones fluids. *The J. Chem. Phys.* **96**, 8639–8640 (1992).
24. YA Lei, T Bykov, S Yoo, XC Zeng, The Tolman Length: Is It Positive or Negative? *J. Am. Chem. Soc.* **127**, 15346–15347 (2005).
25. G Tartero, W Krauth, Markov-chain sampling for long-range systems without evaluating the energy. *J. Chem. Phys.* **161** (2024).
26. G Tartero, W Krauth, Concepts in Monte Carlo sampling. *Am. J. Phys.* **92**, 65–77 (2024).
27. EP Bernard, W Krauth, DB Wilson, Event-chain Monte Carlo algorithms for hard-sphere systems. *Phys. Rev. E* **80**, 056704 (2009).
28. EAJF Peters, G de With, Rejection-free Monte Carlo sampling for general potentials. *Phys. Rev. E* **85**, 026703 (2012).
29. SC Kapfer, W Krauth, Cell-veto Monte Carlo algorithm for long-range systems. *Phys. Rev. E* **94**, 031302 (2016).
30. G Tartero, W Krauth, Concepts in Monte Carlo sampling. *Am. J. Phys.* **92**, 65–77 (2024).
31. P Höllmer, L Qin, MF Faulkner, AC Maggs, W Krauth, JeLLyFysh-Version1.0 — a Python application for all-atom event-chain Monte Carlo. *Comput. Phys. Commun.* **253**, 107168 (2020).